

Atom Resolved Discrimination of Chemically Different Elements on Metal Surfaces

L. Ruan, F. Besenbacher, I. Stensgaard, and E. Laegsgaard

Institute of Physics and Astronomy, Aarhus University, DK-8000 Aarhus C, Denmark

(Received 15 March 1993)

By reversibly manipulating the apex of the tip in a scanning tunneling microscope (STM), we can image either the O or the Cu or Ni atoms in the added rows which constitute the oxygen-induced (2×1) reconstruction of the (110) surfaces of Cu and Ni. This implies that the STM can be used to discriminate between chemically different elements on metal surfaces.

PACS numbers: 61.16.Ch, 68.35.Bs

The fact that distinguishes scanning tunneling microscopy (STM) from other surface-analytical techniques is its demonstrated capability to probe the geometric and electronic structure of surfaces with real-space atomic resolution [1]. Recently, dynamic processes such as adatom diffusion [2], chemical reactions [3], and adsorbate-induced restructuring of surfaces [4,5] have also been studied in real time and space with atomic resolution. Although the STM technique is thus unique in many respects, the extraction of certain types of information is in specific cases less direct than desirable. One of them is the ability to discriminate between chemically different atoms constituting the surface structure.

On selected heteroepitaxially grown semiconductor surface structures, scanning tunneling spectroscopy (STS) and barrier-height measurements have been used to give unprecedented details on the local electronic structure, but only in very few cases is it possible to associate this information with the chemical identity of the images [6,7]. However, STS has had much less impact on the study of metal surfaces, mainly because STS spectra on metal surfaces often show very little structure in the energy range ± 2 V around the Fermi level ϵ_F .

In this Letter, we address the important question of chemical specificity in STM imaging of metal surfaces. It is shown that by reversibly manipulating the chemical identity of the apex of the tunneling tip, we can discriminate between the O and Cu atoms in low-coordinated -Cu-O- rows on Cu(110) and, equivalently, between O and Ni atoms in -Ni-O- rows on Ni(110). Oxygen induces a (2×1) reconstruction on Cu(110), which consists of added rows of -Cu-O- running along the [001] direction, one row for every two $[1\bar{1}0]$ bulk-lattice spacings. By either field desorbing or sputter cleaning the W tip, such that the apex presumably consists of a W atom, the protrusions along the -Cu-O- rows can be associated with the O atoms. Chemisorbing an O atom at the apex of the tip causes the tunneling images to change, and the protrusions along the rows shift to the location of the Cu atoms. In both cases, one observes only one protrusion per -Cu-O- segment, i.e., the other atom seems to be invisible in the STM images. Identical conclusions are obtained for the Ni(110)- (2×1) O surface.

The experiments, all carried out at room temperature (RT), were performed with a fully automated STM [8,9]

for which atomic resolution is obtained on metal surfaces on a routine basis. The tunneling tips were made by electrochemically etching a single-crystal W(001) wire, 0.5 mm diameter, prior to mounting in the UHV STM. The STM images were all acquired in the constant-current model I_t ranging from 0.1 to 4 nA, and the tunneling bias V_t applied to the sample with the tip at virtual ground. The sample preparation and cleaning are described elsewhere [8,9].

Recently, STM studies have established that the formation of the O-induced (2×1) reconstruction on Cu(110) [9-11] and Ni(110) [12,13] proceeds via a novel mechanism, an "added-row" growth mode, in which metal atoms are released from, e.g., step edges and diffuse across terraces and condense with chemisorbed O atoms into low-coordinated -metal-O- added rows running along the [001] direction. The added rows, which nucleate homogeneously on the terraces, are very mobile at RT, but a strong one-dimensional bond acts along the rows to keep them intact as they diffuse across the terrace. As the density of the added rows increases, they agglomerate into (2×1) -reconstructed anisotropic islands, with a long (short) coherence length in the [001] ($[1\bar{1}0]$) directions, as indicated in Fig. 1.

In Fig. 2 are shown STM images of (2×1) O added rows and/or domains coexisting with clean (1×1) regions on Cu(110). In this case, the surface was exposed to 4 langmuir ($1 \text{ L} = 10^{-6} \text{ torrsec}$) of oxygen at RT, and the (2×1) O structure covers approximately 20% of the surface. In the O-covered region, the periodicity of the pro-

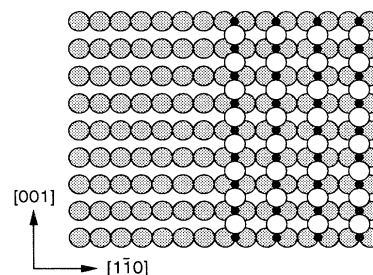


FIG. 1. An atomistic model of the O-induced [001]-directed added rows on Cu(110). The small black circles represent the O atoms, whereas the large white and grey circles represent the Cu atoms in the first and second layer, respectively.

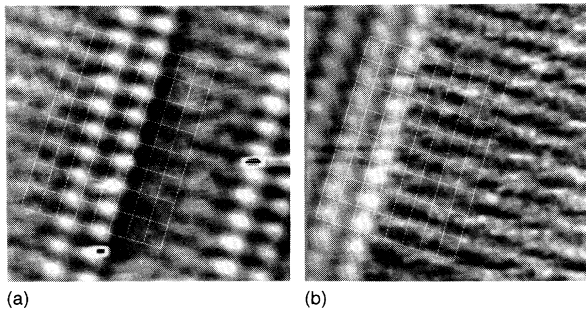


FIG. 2. STM images ($40 \times 41 \text{ \AA}^2$) of the $(2 \times 1)\text{O}$ structure coexisting with the bare $\text{Cu}(110)$ surface obtained with a clean W tip (a) and after chemisorption of an O atom at the apex of the tip (b). Both images are recorded with $V_t = 50 \text{ mV}$ and $I_t = 4 \text{ nA}$. Surface protrusions are white, while depressions are black. The grids indicate the positions of the Cu atoms in the (1×1) Cu layer underlying the added $-\text{Cu-O}-$ rows. In (a) the protrusions of the added rows are in line with the close-packed rows of the underlying $\text{Cu}(1 \times 1)$ surface, whereas in (b) they are out of registry.

trusions is $5.0 \pm 0.1 \text{ \AA}$ and $3.6 \pm 0.1 \text{ \AA}$ along the $[1\bar{1}0]$ and $[001]$ directions, respectively, consistent with a local $(2 \times 1)\text{O}$ reconstruction with O and Cu densities of $\Theta_{\text{O}} = 0.5 \text{ ML}$ (monolayer) and $\Theta_{\text{Cu}} = 0.5 \text{ ML}$. From the literature, there is overwhelming evidence that O is located in the long-bridge position, i.e., in between two Cu atoms along the $[001]$ direction [14], as depicted in Fig. 1. Since the periodicity along this direction of the added rows is 3.6 \AA , the observed protrusions along the rows have to be identified with either the O or the Cu atoms.

In previous STM studies on the $\text{Cu}(110)-(2 \times 1)\text{O}$ [9–11] and $\text{Ni}(110)-(2 \times 1)\text{O}$ [12] phases, the protrusions along the $[001]$ direction were reported earlier in line with the $[1\bar{1}0]$ rows of the underlying (1×1) surface (see Fig. 1) and thus associated with the O atoms, or they were out of “registry” and thus associated with the Cu or Ni atoms.

To further study these conflicting observations, we decided to investigate the influence of the chemical identity of the apex atoms of the tip on the STM images. First, we cleaned the tip by field desorption, i.e., the tunneling voltage is ramped up to 5–10 V in 1 msec. This generally causes the transfer of material from the tip to the surface and thus has to be done in an area away from the scanning area [15]. With such a supposedly “clean tip,” the tunneling behavior was reproducible and stable, at least for some time, and the protrusions of the (2×1) phase were in line with the $[1\bar{1}0]$ rows of the clean surface [Fig. 2(a)]. Thus with a clean “W tip,” we image the O atoms.

Letting tiny amounts of oxygen into the chamber (0.05 L) or by just scanning the $(2 \times 1)\text{O}$ surface for a while, a sudden uncontrollable tip change occurs, and, correlated with the tip change, the protrusions of the (2×1) structure change to be out of registry with the close-packed

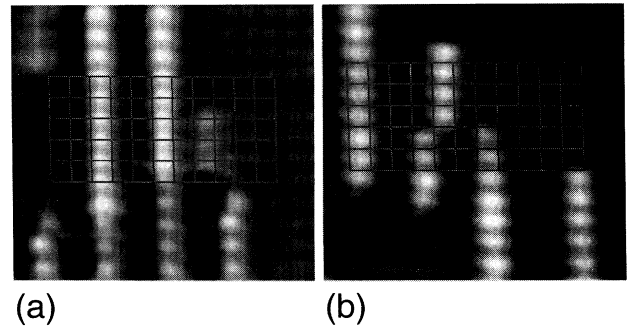


FIG. 3. STM images ($37 \times 47 \text{ \AA}^2$) of the added $-\text{Ni-O}-$ $[001]$ rows on $\text{Ni}(1 \times 1)$ obtained with a clean W tip (a) and after chemisorption of an O atom at the apex of the tip (b). For both images, $V_t = 10 \text{ mV}$ and $I_t = 1 \text{ nA}$. The grids indicate the positions of the Ni atoms in the $(1 \times 1)\text{Ni}$ layer underlying the added $-\text{Ni-O}-$ rows. In (a) the protrusion of the added rows are in line with the close-packed rows of the underlying $\text{Ni}(1 \times 1)$ surface, whereas in (b) they are out of registry.

$[1\bar{1}0]$ rows of the clean Cu surface [Fig. 2(b)]. We tentatively suggest that the tip change is associated with the binding of an O atom at the apex of the tip. Thus with an “O tip,” we image the Cu atoms as protrusions. Cleaning the tunneling tip again, as described above, the protrusions shift back in line with the $[1\bar{1}0]$ rows, and the O atoms are imaged again. We therefore conclude that by reversibly manipulating the apex of the tunneling tip to have either a W atom or an O atom at the apex, one images the O and the Cu atoms, respectively, in the $-\text{Cu-O}-$ rows, i.e., we can discriminate chemically different elements such as O and Cu with the STM.

Also for the case of O-induced reconstruction on $\text{Ni}(110)$, the chemical identity of the tunneling tip appears to have a strong influence on the STM images. Exposing the $\text{Ni}(110)$ surface to 0.4 L of oxygen, a few $[001]$ -directed $-\text{Ni-O}-$ added rows are formed on the $\text{Ni}(1 \times 1)$ surfaces, as seen from the STM images in Fig. 3. When more are formed, these added rows will nucleate together in islands which locally have a (3×1) or (2×1) periodicity with $\Theta_{\text{O}} = \frac{1}{3}$ or $\frac{1}{2} \text{ ML}$ and $\Theta_{\text{Ni}} = \frac{1}{3}$ or $\frac{1}{2} \text{ ML}$, respectively [12]. For these structures, O is located in the long-bridge position [16]. With a tunneling tip which is cleaned by field desorption, we see that the protrusions of the $-\text{Ni-O}-$ added rows are lying in line with the close-packed $[1\bar{1}0]$ rows of the $\text{Ni}(1 \times 1)$ crystal [Fig. 3(a)]. However, with a tip which has been exposed to oxygen and which is likely to have an O atom adsorbed at the apex, we observe just the opposite, i.e., the protrusions are lying in between the close-packed Ni rows [Fig. 3(b)]. This implies that with the W tip we are imaging the O atoms, whereas with the O tip we image the Ni atoms. Apparently, it is again possible to perform atom resolved discrimination between chemically different elements.

For the results presented above, it is important to

resolve the $(2\times 1)/(3\times 1)$ added-row O structures simultaneously with at least the close-packed rows of the bare (1×1) surface to have a reference frame. This is best obtained for $I_t \approx 0.5\text{--}4$ nA and $V_t \approx 10\text{--}100$ mV, and the results are found to be independent of the polarity of V_t in this range. At higher V_t , we can easily resolve the (2×1) O structure, but it becomes increasingly difficult simultaneously to resolve the (1×1) structure [17].

How are these results to be understood? The tunneling current depends exponentially on the distance between the tip and the surface, typically varying about an order of magnitude for a change of only 1 Å in this distance. Thus the tunneling process is localized to the very end of the tip, resulting in atomic resolution. Generally, the STM images represent a convolution not only of the surface geometrical and electronic structure, but also the tip electronic structure may contribute. However, for a clean W tip, it is often reported, or implicitly assumed, that the electronic structure of the tip is relatively unimportant and does not influence the tunneling behavior significantly [18]. Then, for the case of weak interactions between the tip and the sample, the STM images have, in a Bardeen perturbative-transfer Hamiltonian approach, an interpretation as contours of constant local density of states (LDOS) at the Fermi level of the sample surface [19]. On clean metal surfaces, these contours are to a first approximation similar to the contours of the total electronic-charge density, and the STM images can be interpreted as topographic maps [19].

Adsorbates on metal surfaces will generally induce a change in the LDOS near ϵ_F , and for the perturbative jellium approach developed by Lang [20], the adsorbate will appear as protrusions (holes) if it adds to (depletes) the LDOS at ϵ_F . According to Lang's calculations, a small electronegative atom such as O makes a negative contribution to the state density at the Fermi level, in good accordance with the experimental finding that for the chemisorption of O on Ni(111) [21] and Ni(100) [4,5], the O atoms are imaged as holes located in threefold and fourfold hollow sites on the unreconstructed surface, respectively. Although Lang's calculations are not directly applicable to the present condition, where strong anisotropic metal-O bonds are formed along the -metal-O-rows, one would still expect to image the metal atoms, i.e., the Cu or Ni atoms, as protrusions. This is supported by the more elaborate simulation of STM images, based on the first-principle local-density approach by Tsukada and Shimizu [22]. They used a W cluster as the tip and slab models for the surface for the calculation of the surface electronic/geometrical structure and found for -metal-O- rows on Ag(110) and Cu(110) that the metal atoms are imaged as protrusions. Thus it is difficult to explain the present findings in a picture based on conventional perturbative STM theories, for which the interaction between the tip and the sample is implicitly assumed to be weak.

One way to tentatively explain the experimental

findings is to invoke tip-surface interactions, e.g., the tunneling may occur through some kind of weak chemical interaction or bond. Tip-sample interactions may cause a W tip to form a stronger "chemical bond" with the O atoms along the rows than with the metal (Cu or Ni) atoms, whereas an O tip may form a stronger "chemical bond" to the Cu or Ni atoms than to the O atoms. By manipulating the chemical identity of the tip apex, the formation of a "chemical bond" between the tip and the sample may increase or decrease the density of states at ϵ_F and thereby I_t , since antibonding states, resulting from tip-surface atom interactions, are either shifted up to or pushed away from ϵ_F . Theoretical calculations are called for to investigate these speculations.

Doyen [23] has previously pointed out that tip-sample interactions are important, and for clean metal surfaces, image-inversion effects may arise, i.e., the interstitial regions rather than the substrate atoms appear as maxima in the constant-current images. To exclude image-inversion effects [24] and to further confirm the above results, we show in Fig. 4 STM images of coexisting $c(2\times 2)$ S and (2×1) O phases, recorded during the STM studies of the reaction between H_2S and O on Cu(110) [3], imaged with a W tip [Fig. 4(a)] and an O tip [Fig. 4(b)], respectively. In these cases, the $c(2\times 2)$ S structure is used as a reference frame. Chemisorption of S on Cu(110) results in the formation of $c(2\times 2)$ S overlayer structures on the unreconstructed Cu(110) surface, and S atoms are imaged as protrusions in the twofold hollow site on the (1×1) surfaces [25], consistent with Lang's predictions [20], independent of the tip state, and at tunneling conditions identical to those used for the results of Figs. 2 and 3. From Fig. 4 it is seen that one again images either the O atoms [Fig. 4(a)] or the Cu atoms [Fig. 4(b)]. In this case, it is easier to resolve the reference frame, $c(2\times 2)$ S, simultaneously with the (2×1) O structure, and for tunneling parameters $I_t = 0.5\text{--}1.0$ nA and $V_t = 10\text{--}500$ mV,

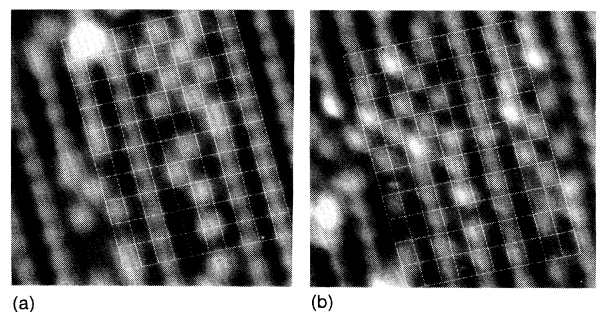


FIG. 4. Two STM images (44×46 Å²) of (2×1) O and $c(2\times 2)$ S coexisting phases on Cu(110) obtained with a clean W tip (a) and after chemisorption of an O atom at the apex of the tip (b), recorded with $V_t = 500$ mV and $I_t = 0.5$ nA. The grids indicate the positions of the Cu atoms in the (1×1) Cu layer underlying both structures. The images are recorded during the STM studies of the reaction between H_2S and O on Cu(110) [3].

the registry does not change.

Few other studies have dealt with the influence on the tunnel current of foreign atoms on the tip [26] in a systematic manner. For a heteroepitaxial system, Ag on Si(111), a strong asymmetry in STS was observed, i.e., absence of atomic resolution for filled states of the sample and at the same time atomic resolution for the empty states. Theoretical calculations by Lang suggest that the adsorption of an electronegative atom on the probe tip accounts for the findings [26]. However, the existence of a foreign atom at the tip apex did not lead to any new way of discriminating between the Ag and Si atoms in the unit cell.

In conclusion, we have addressed the important issue of the determination of the chemical specificity of surfaces with STM. It is shown that by reversibly manipulating the apex of the tip to have either a W atom or an O atom, we can discriminate between O and Cu or Ni atoms in -Cu-O- or -Ni-O- rows. These observations emphasize the importance of the chemical identity of the tip-apex atom and have important implications for a number of experiments routinely performed in scanning tunneling microscopy, since often during scanning of, e.g., adsorbate-covered surfaces, the tip may pick up a chemically reactive adsorbate such as O and S. This may indeed explain the surprising contrast mechanism in STM studies on a PtNi alloy surface [27] under special uncontrolled tip conditions, and between Au and Ni [28] and Fe and Cu [29] on heteroepitaxially grown surfaces. In closing, selective adsorption of chemically reactive foreign atoms may open new possibilities in scanning tunneling microscopy.

We gratefully acknowledge the financial support from the Danish Research Councils through the "Centre for Surface Reactivity" and the Knud Højgaard Foundation.

- [1] G. Binnig, H. Rohrer, Ch. Gerber, and E. Weibel, *Phys. Rev. Lett.* **49**, 57 (1982).
- [2] E. Ganz, S. K. Theiss, I. Hwang, and J. Golovchenko, *Phys. Rev. Lett.* **68**, 1567 (1992); R. M. Feenstra, A. J. Slavin, G. A. Held, and M. A. Lutz, *Phys. Rev. Lett.* **66**, 3257 (1991).
- [3] L. Ruan, F. Besenbacher, I. Stensgaard, and E. Laegsgaard, *Phys. Rev. Lett.* **69**, 3523 (1992).
- [4] J. Wintterlin and R. J. Behm, in *Scanning Tunneling Microscopy I*, edited by H.-J. Güntherrodt and R. Wiesendanger, Springer Series in Surface Sciences Vol. 20 (Springer-Verlag, Berlin, 1992), Chap. 4.
- [5] F. Besenbacher and I. Stensgaard, in "The Chemical Physics of Solid Surfaces and Heterogeneous Catalysis," edited by D. A. King and D. P. Woodruff (Elsevier, Amsterdam, to be published), Vol. 7, Chap. 15.
- [6] R. M. Tromp, *J. Phys. Condens. Matter* **1**, 10211 (1989).
- [7] G. Binnig and H. Rohrer, *Surf. Sci.* **126**, 236 (1983).
- [8] E. Laegsgaard, F. Besenbacher, K. Mortensen, and I. Stensgaard, *J. Microsc.* **152**, 663 (1988); F. Besenbacher, F. Jensen, E. Laegsgaard, K. Mortensen, and I. Stensgaard, *J. Vac. Sci. Technol. B* **9**, 874 (1991). The microscope is a prototype of RASTERSCOPE 3000 from DME, Herlev, Denmark.
- [9] F. Jensen, F. Besenbacher, E. Laegsgaard, and I. Stensgaard, *Phys. Rev. B* **41**, 10233 (1990).
- [10] D. J. Coulman, J. Wintterlin, R. J. Behm, and G. Ertl, *Phys. Rev. Lett.* **64**, 1761 (1990).
- [11] Y. Kuk, F. M. Chua, P. J. Silverman, and J. A. Meyer, *Phys. Rev. B* **41**, 12393 (1990); F. M. Chua, Y. Kuk, and P. J. Silverman, *Phys. Rev. Lett.* **63**, 386 (1989).
- [12] L. Eierdal, F. Besenbacher, E. Laegsgaard and I. Stensgaard, *Ultramicroscopy* **42-44**, 505 (1992); (to be published).
- [13] O. Haase, R. Koch, M. Borbonus, and K. H. Rieder, *Phys. Rev. Lett.* **66**, 1725 (1991).
- [14] S. R. Parkin, H. C. Zeng, M. Y. Zhou, and K. R. Mitchell, *Phys. Rev. B* **41**, 5432 (1990).
- [15] Another way of cleaning the tip is by sputtering; i.e., the tip, placed 10 μm from the sample at the edge of the crystal, is biased 2 kV negatively with respect to the sample and Ne is let in to a pressure of 3×10^{-4} mbar. Field-emitted electrons ionize the Ne, creating positive Ne ions which are then accelerated towards the tip and sputter clean it.
- [16] G. Kleinle, J. Wintterlin, G. Ertl, R. J. Behm, F. Jona, and W. Moritz, *Surf. Sci.* **225**, 171 (1990).
- [17] While the corrugation along the added rows ($\approx 0.2 \text{ \AA}$) is fairly insensitive to V_t , the apparent height of the added rows above the (1×1) terraces depends on V_t . For the O tip the added rows are nearly coplanar and sometimes even below the (1×1) terrace at low V_t , whereas for the clean W tip, the apparent height of the added rows above the (1×1) terrace is significantly larger and always positive.
- [18] J. E. Demuth, U. Koehler, and R. J. Hamers, *J. Microsc.* **152**, 299 (1988); R. J. Hamers, R. M. Tromp, and J. E. Demuth, *Phys. Rev. Lett.* **56**, 1972 (1986).
- [19] J. Tersoff and D. R. Hamann, *Phys. Rev. Lett.* **50**, 1998 (1983); J. Tersoff, *Phys. Rev. B* **41**, 1235 (1990).
- [20] N. D. Lang, *Phys. Rev. Lett.* **56**, 1164 (1986); *Comments Condens. Matter Phys.* **14**, 253 (1989).
- [21] L. Olesen, F. Besenbacher, I. Stensgaard, and E. Laegsgaard (to be published).
- [22] M. Tsukada, T. Shimizu, S. Watanabe, N. Isshiki, and K. Kobayashi, *Jpn. J. Appl. Phys.* (to be published).
- [23] G. Doyen, in *Scanning Tunneling Microscopy II*, edited by H.-J. Güntherrodt and R. Wiesendanger, Springer Series in Surface Sciences Vol. 28 (Springer-Verlag, Berlin, 1992), Chap. XX.
- [24] The only way in which image inversion may be of concern in Figs. 2(b) and 3(b) is if the (1×1) Cu or Ni surfaces are image inverted exclusively. This seems highly unlikely, since one would expect that the coexisting -Cu-O-Cu- or -Ni-O-Ni- added rows should also be inverted and/or influenced.
- [25] F. Besenbacher, I. Stensgaard, L. Ruan, J. K. Nørskov, and K. W. Jacobsen, *Surf. Sci.* **272**, 334 (1992); I. Stensgaard, L. Ruan, F. Besenbacher, F. Jensen, and E. Laegsgaard, *Surf. Sci.* **269/270**, 81 (1992).
- [26] R. M. Tromp, E. J. van Loenen, J. E. Demuth, and N. D. Lang, *Phys. Rev. B* **37**, 9042 (1988).
- [27] M. Schmid, H. Stadler, and P. Varga (to be published).
- [28] L. Pleth Nielsen, F. Besenbacher, E. Laegsgaard, and I. Stensgaard (to be published).
- [29] D. D. Chambliss, R. J. Wilson, and S. Chiang, *J. Vac. Sci. Technol. A* **10**, 1993 (1992).

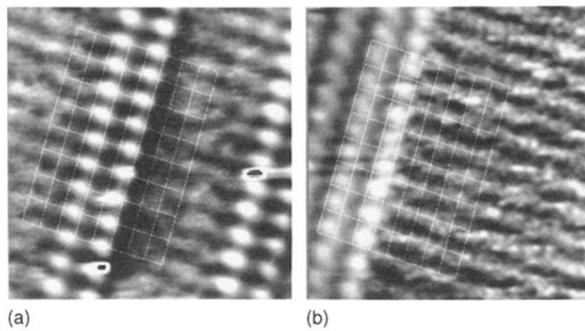


FIG. 2. STM images ($40 \times 41 \text{ \AA}^2$) of the $(2 \times 1)\text{O}$ structure coexisting with the bare Cu(110) surface obtained with a clean W tip (a) and after chemisorption of an O atom at the apex of the tip (b). Both images are recorded with $V_t = 50 \text{ mV}$ and $I_t = 4 \text{ nA}$. Surface protrusions are white, while depressions are black. The grids indicate the positions of the Cu atoms in the (1×1) Cu layer underlying the added -Cu-O- rows. In (a) the protrusions of the added rows are in line with the close-packed rows of the underlying Cu(1×1) surface, whereas in (b) they are out of registry.

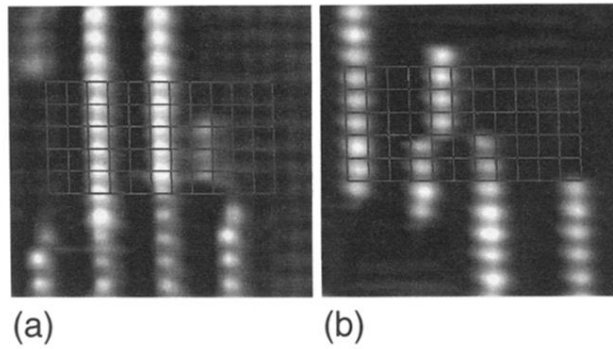


FIG. 3. STM images ($37 \times 47 \text{ \AA}^2$) of the added $-\text{Ni-O}-$ [001] rows on $\text{Ni}(1 \times 1)$ obtained with a clean W tip (a) and after chemisorption of an O atom at the apex of the tip (b). For both images, $V_t = 10 \text{ mV}$ and $I_t = 1 \text{ nA}$. The grids indicate the positions of the Ni atoms in the (1×1) Ni layer underlying the added $-\text{Ni-O}-$ rows. In (a) the protrusion of the added rows are in line with the close-packed rows of the underlying $\text{Ni}(1 \times 1)$ surface, whereas in (b) they are out of registry.

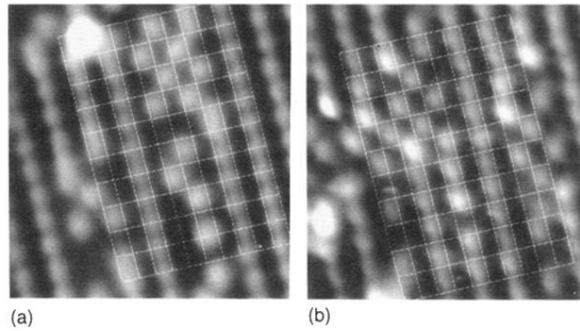


FIG. 4. Two STM images ($44 \times 46 \text{ \AA}^2$) of $(2 \times 1)\text{O}$ and $c(2 \times 2)\text{S}$ coexisting phases on $\text{Cu}(110)$ obtained with a clean W tip (a) and after chemisorption of an O atom at the apex of the tip (b), recorded with $V_t = 500 \text{ mV}$ and $I_t = 0.5 \text{ nA}$. The grids indicate the positions of the Cu atoms in the (1×1) Cu layer underlying both structures. The images are recorded during the STM studies of the reaction between H_2S and O on $\text{Cu}(110)$ [3].